J Bioenerg Biomembr (2008) 40:551–559
DOI 10.1007/s10863-008-9189-z

Conformational changes in the *Escherichia coli* ATP synthase *b*-dimer upon binding to F_1-ATPase

Tarek M. Zaida · Tassilo Hornung · Oleg A. Volkov · Andrea D. Hoffman · Susan J. Pandey · John G. Wise · Pia D. Vogel

Received: 15 August 2008 / Accepted: 24 November 2008 / Published online: 14 January 2009

Abstract Conformational changes within the subunit *b*-dimer of the *E. coli* ATP synthase occur upon binding to the F_1 sector. ESR spectra of spin-labeled *b* at room temperature indicated a pivotal point in the *b*-structure at residue 62. Spectra of frozen *b* ± F_1 and calculated interspin distances suggested that where contact between b_2 and F_1 occurs (above about residue 80), the structure of the dimer changes minimally. Between *b*-residues 33 and 64 inter-subunit distances in the F_1-bound *b*-dimer were found to be too large to accommodate tightly coiled coil packing and therefore suggest a dissociation and disengagement of the dimer upon F_1-binding. Mechanistic implications of this "bubble" formation in the tether domain of ATP synthase b_2 are discussed.

Keywords Coiled coil · ESR · Spin-labeling · ATPase · Conformational changes · b-dimer · External stalk

This work was supported by grant from the National Science Foundation (MCB 0415713) to PDV

T. M. Zaida · T. Hornung · O. A. Volkov · A. D. Hoffman · S. J. Pandey · J. G. Wise · P. D. Vogel (✉)
Department of Biological Sciences,
Southern Methodist University,
6501 Airline Rd.,
Dallas, TX 75275, USA
e-mail: pvogel@smu.edu

Present address:
T. Hornung
Biomedicine and Biotechnology, School of Life Sciences,
Arizona State University,
Tempe, AZ, USA

Abbreviations

MTS-SL	1-oxyl-2,2,5,5-tetramethyl-3-pyrroline-3-methyl) methanethiosulfonate
IAAT	spin label, 4-(2-Iodoacetamido)-2,2,6,6-tetramethylpiperidine 1-oxyl
DEER	double electron-electron resonance spectroscopy

Introduction

F_oF_1 ATP synthase is a widely found enzyme that is responsible for the bulk of ATP production in aerobic and photosynthetic organisms. The highly asymmetric enzyme consists in its simplest bacterial form of 8 different polypeptides with the subunit stoichiometry $\alpha_3\beta_3\gamma\delta\varepsilon$ in the peripheral F_1 that contains the nucleotide binding and catalytic sites for ATP synthesis and hydrolysis, and $ab_2c_{10\text{-}15}$ in the membrane-embedded F_o-part that constitutes the proton-translocation apparatus (for recent review see (Vik 2007)).

Great effort has been made over the last few years to determine the structure and function of the external stalk of the F_oF_1-ATP synthase. This external stalk is thought to bind the F_1 and the F_o sectors together and is thought to be either a rigid stator as indicated by the X-ray structural model of mitochondrial ATPase (Dickson et al. 2006; Walker and Dickson 2006) or a flexible connector that may allow elastic coupling between the differential movement of the proton-driven c-ring rotation to the rotation of the inner shaft consisting of subunits γ and ε (Junge et al. 2001). Especially, the homodimeric *b*-subunits from eubacterial ATP synthases have been thought to be highly flexible since deletions and insertions of amino acid sequences into the *b*-subunit allowed formation of functional enzyme

(Sorgen et al. 1998; Sorgen et al. 1999), even if these deletions resulted in unequal length *b*-dimers interacting with the F_1-part (Bhatt et al. 2005; Grabar and Cain 2003).

Much work has been done using a soluble mutant of the *Escherichia coli b*-dimer that is lacking its membrane spanning domain and was first introduced by the Dunn lab. In addition to cross-linking studies that showed inter-*b* cross links as well as cross links between *b* and subunits located in F_1 (for review see (Dunn et al. 2000a)), the Dunn lab was successful in obtaining an X-ray crystallographic model of a monomeric portion of *E. coli b* (Del Rizzo et al. 2002). Upon visual inspection of the X-ray structural model and later due to a variety of disulfide cross-link experiments these authors suggested that the dimerization domain of the *b*-dimer forms a right-handed coiled coil (Bi et al. 2008; Del Rizzo et al. 2006; Wood and Dunn 2007) with a staggered off-set of the two amino acid chains by either 4, 7 or 11 amino acids, resulting in asymmetric interaction of the *b*-dimer with the F_1-part. As of yet, no stable dimeric right handed coiled coils have been observed in any protein by any structural biophysical technique.

Very recent low-resolution X-ray and NMR studies on the *b*-dimer and a *b*-*δ* complex do not support the staggered arrangement suggested by Dunn and no overhang was observed (R. Priya, V. S. Tadwal, M. W. Roessle, S. Gayen, C. Hunke, W. C. Peng, J. Torres and G. Grüber, "Low resolution structure of subunit *b* (*b22–156*) of *Escherichia coli* F_1F_O-ATP synthase in solution and the *b*-δ assembly" (2008), *J. Bioenerg. Biomembr.,* Jul 31. [Epub ahead of print]). These same authors reported non-Cu-catalyzed disulfide formation of the naturally occurring cysteine 21 of the *E. coli b* protein which is highly suggestive of a non-staggered arrangement of b_2 close to the N-terminus. It should be noted that this latter observation was made for the complete b_2 but in the absence of subunits *a* and *c*.

Our lab has recently presented evidence that the soluble *b*-dimer from *E. coli* can stably exist in a more traditional left-handed coiled coil packing. This conclusion was based on structure prediction and molecular modeling that were first tested on known left-handed coiled coil structures (Wise and Vogel 2008). The same methods were then used to build a model of the soluble *b*-dimer. The generated left-handed coiled coil b_2 model was validated through the use of ESR spectroscopy and site-directed spin labeling. This technique allowed us to determine interspin distances between introduced spin-labels at equivalent amino acid positions in the *b*-dimer (Hornung et al. 2008). Using similar methods with spin-labels possessing different characteristics (length of tether, flexibility), we were previously able to map the approximate interactions between soluble, truncated b_2 and soluble F_1 (Motz et al. 2004). These experiments suggested that tight interaction with F_1 started C-terminal of about amino acid 80 of the *b*-dimer. Theoretically, incorporation of these results with our modeling studies of b_2 leaves approximately 4-5 heptad coiled coil units closely associated with F_1 (residues ~80–116) and a further 6–7 heptad units N-terminally (residues 31− ~ 79) that are not closely associated with F_1 subunits.

These results on the *b*-dimer structure discussed above have been restricted to the soluble, truncated b_2 in the absence of the rest of the enzyme. Steigmiller *et al.* (2005), however, reported that five spin-labels introduced into cysteine mutations in b_2 in the F_oF_1 holoenzyme within the tether region of *b* (between the membrane and residue 65) showed interspin-inter-*b*-distances of 29Å each. They used pulsed ESR techniques in their approach that allowed them to detect and determine inter-spin distances larger than can be detected using the continuous wave ESR we have used. The spin labels in their studies were positioned at residues 40, 51, 53, 62 and 64. Interspin distances of 29Å are inconsistent with tight coiled coil interactions in this amino acid range and therefore were in conflict with the modeling and interspin distances that we had obtained and reported for soluble *b* (Hornung et al. 2008; Wise and Vogel 2008).

In this present paper we present results of experiments that took our earlier structural work on the *b*-dimer an additional step further. We used a subset of the cysteine mutant *b*-proteins that were employed in our earlier studies to determine the structure of the *b*-dimer in the presence of added soluble F_1. ESR spectra of the subunit *b*-dimer in the presence and absence of F_1 were compared at room temperature and in frozen solution. We observed differences in the interspin distances in the tether region of the *b*-dimer in the presence of the F_1-ATPase that suggested a structure for the *b* dimer consistent with the data reported by Steigmiller *et al.* (Steigmiller et al. 2005). We present here that those parts of the *b*-dimer that we showed earlier to be closely interacting with F_1 (at residues greater than ~80) (Motz et al. 2004) as well as a significant part of *b* not yet shown to directly interact with F_1 (residues 65–79) most likely retain their unperturbed left-handed coiled coil packing when in complex with F_1, while binding to F_1 results in a dissociation and disengaging of the predicted coiled coil within the tether region of the *b*-dimer. In the absence of other F_o subunits, at amino acid position 31 of *b*, which is close to the membrane, tight packing interactions seem to resume. These results are consistent with a parallel arrangement of the *b*-dimer within the membrane as observed in studies presented in (Dmitriev et al. 1999) and the ability of the naturally occurring cysteines at position 21 to form Cu-independent cross-links ((R. Priya, V. S. Tadwal, M. W. Roessle, S. Gayen, C. Hunke, W. C. Peng, J. Torres and G. Grüber, "Low resolution structure of subunit *b* (*b22–156*) of *Escherichia coli* F_1F_O-ATP synthase in solution and the *b*-δ

assembly" (2008), *J. Bioenerg. Biomembr.,* Jul 31. [Epub ahead of print]).

Experimental procedures

Mutagenesis and expression of subunit b The single cysteine mutations of subunit *b* were obtained by standard molecular biology techniques and as described in (Hornung et al. 2008). Cysteine mutations of the truncated subunit *b*-dimer were expressed in *E. coli* strain JM109 from derivatives of plasmid pDM3 (McLachlin and Dunn 1997). Protein purification and chemical modification with MTS-spin label (1-oxyl-2,2,5,5-tetramethyl-3-pyrroline-3-methyl) methanethiosulfonate) was as described in (Hornung et al. 2008). The degree of spin labeling of the samples was usually between 70 and 90%. Protein purity was verified using SDS-PAGE (Laemmli 1970). Usual concentrations of spin-labeled *b*-dimer were ranging from 10μM to 100μM.

Expression and purification of F_1-ATPase Wild-type F_1 was expressed from SWM1 and purified essentially as described in (Wise 1990). The purity of protein was determined by SDS-PAGE (Laemmli 1970). Protein fractions were collected and concentrated using Centricon 30 ultra-concentrators (Amicon). ATP hydrolysis activities were detected as described (Wise 1990) using the phosphate detection method developed by (Taussky and Shorr 1953). Concentrated F_1 was stored at −80°C for later use in ESR experiments.

ESR-Measurements All ESR-spectra were acquired at a Bruker EMX 6/1 equipped with a high sensitive cavity. All ESR-measurements were performed in the X-band mode with a modulation amplitude of 1 G. The receiver gain was adjusted to protein concentrations. Microwave power was set to 12.5mW for measurements at room temperature (294K) or 4mW for frozen solution ESR measurements at 223K (for determining intermolecular distances). The buffer used for ESR measurements was composed of 50mM TrisHCl, 7mM $MgSO_4$ and 10mM KCl, pH7.5. For those experiments that included F_1-ATPase, a molar ratio of 1:1.2 (b_2: F_1) was employed to ensure that all *b*-dimer was bound to F_1. DTT was removed from the enzyme prior to mixing it with b_2. Frozen spectra were analyzed using a convolution algorithm assuming a Gaussian distribution of distances as described in detail in (Hustedt et al. 2006) and that was developed according to procedures described in (Steinhoff et al. 1997) and (Rabenstein and Shin 1995).

Molecular modeling Modeling of the coiled coil *b*-dimer and the spin labeled cysteinyl residues was as described in (Hornung et al. 2008; Wise and Vogel 2008) and is only depicted in an abbreviated form here for better understanding: The structure of the MTS spin-labeled cysteine residues was drawn using Molecular Simulations InsightII program (v. 2000.1). Quantum mechanical simulations of the spin-labeled derivatized cysteinyl residues were performed to locate equilibrium geometries using the program GAMESS (Schmidt et al. 1993) and an unrestricted Hartree-Fock 6–31 basis set. Partial atomic charges for the residues were calculated. The QM/MM-derived structures were visualized using Molden (Schaftenaar and Noordik 2000). To model the *b*-dimer coiled coil domains, prediction of heptad repeats in the subunit *b* amino acid sequence was performed using Paircoil2 (McDonnell et al. 2006). Visualization and analysis of the protein structures was accomplished using Visual Molecular Dynamics (VMD) program suite (Humphrey et al. 1996). To model coiled coil structures, seven known left-handed, dimeric coiled coil entries in the Protein Data Bank were analyzed using the Paircoil2 program and Tcl/Tk (Ousterhout 1994) and Python (Sanner 1999) scripting interfaces within VMD to generate a set of ideal distance and dihedral restraints for dimeric left-handed coiled coil domains. These restraint sets were then used in *ab initio* simulated annealing (SA) experiments with the XPLOR-NIH suite-versions 2.11 through 2.18 (Schwieters et al. 2003). The experimentally generated left-handed coiled coil structures for subunit *b* ranged from residue 31 to residue 122. Upon refinement, a set of acceptable structures was identified and specific residues of subunit *b* were individually substituted with the spin-labeled cysteine residue described above and interspin distances were determined. The calculations were performed on a 68-CPU Linux computing cluster with Scientific Linux 5.0 operating systems.

Results

Global effects of F_1-binding on the b-dimer structure ESR experiments at room temperature and in liquid solution often allows the observation of conformational transitions within the structure of the labeled protein, usually observed by changes in the mobility of the radical. Figure 1a and b show room temperature ESR experiments of a set of MTS-spin labeled soluble *b*-dimers where the membrane anchor had been truncated (McLachlin and Dunn 1997) in the presence or absence of soluble F_1. In Figure 1a the corresponding spectra of mutations within most of the tether region of the protein are shown (residues 33 to 64) while Fig. 1b presents the ESR spectra of mutants within the dimerization domain *of b* and further extended towards the C-terminus of the protein (through residue

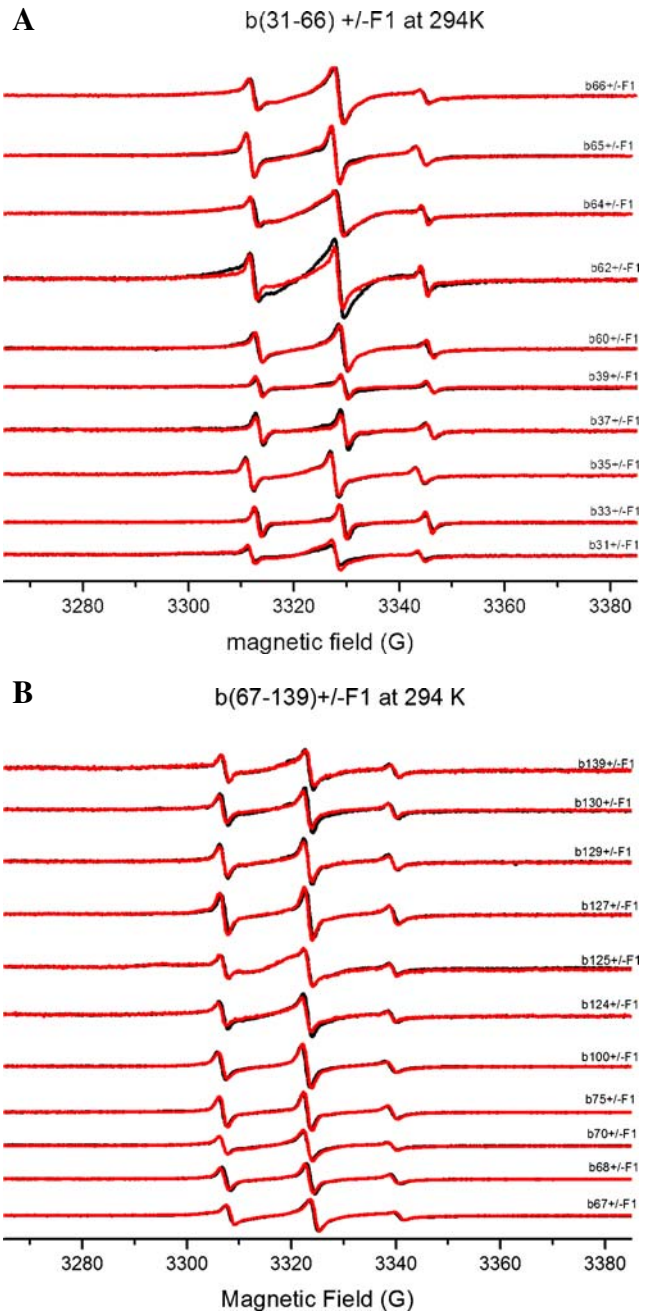

Fig. 1 ESR-spectra acquired in liquid solution of selected cysteine mutations in the E. coli F_oF_1-ATP synthase subunit b-dimer in the presence and absence of soluble F_1-ATPase. **a** ESR spectra of spin-labeled b-mutants within the tether domain of the protein; **b** ESR spectra of spin-labeled b-mutants within the dimerization domain and towards the C-terminus acquired at 294 K. The black lines represent the ESR spectra of the b-dimer alone, the overlaid red spectra were obtained after addition of a 1.2 fold excess of F_1-ATPase over b-dimer. The concentration of soluble subunit b-dimer was between 10 and 100 μM. The corresponding spectra (+/− F_1) were normalized for their b-protein concentration to cancel out effects of dilution upon F_1 addition. Conditions for acquiring the ESR spectra are given in Experimental procedures. Residue positions are given in the Figure

139). The ESR spectra resulting from MTS-spin-labeled soluble, truncated b_2 are shown in black and the spectra of identically labeled b_2 in complex with F_1 are overlaid in red. The individual spectra were normalized for the respective *b*-protein concentration to accommodate dilution effects upon addition of F_1-ATPase. The experimental conditions, i.e. protein concentrations and F_1 to b_2-ratio, were chosen according to measurements described in (Motz et al. 2004) where we showed through two-dimensional gel electrophoresis that complexation of b_2 to F_1 takes place when about 1.2mol of b_2 are incubated with 1 mole of F_1. Except for the spectra of *b* labeled at amino acid residue 62, no significant change in the shape of the spectra was observed, suggesting that binding of F_1 to b_2 did not result in major changes of the spin labels' mobility in most amino acid positions. This result is different from earlier measurements where we used the more flexible IAAT spin label (4-(2-Iodoacetamido)-2,2,6,6-tetramethylpiperidine 1-oxyl). IAAT spin label is highly flexible and results in very sharp ESR spectra even when bound to the *b*-dimer that correlate to relatively short rotational correlation times see (Motz et al. 2004). Upon binding of the IAAT-spin-labeled b_2 to F_1 a broadening of the ESR spectral line shape was observed, consistent with the loss of label mobility (Motz et al. 2004) due to an increased rotational correlation time of the b_2-F_1 complex as compared to b_2 alone. The difference observed in the experiments presented here and when using MTS-spin label is likely due to the overall greater rigidity of the MTS-spin label and its overall decreased mobility that may not allow MTS-SL to report on overall loss of complex mobility as does IAAT-SL. Such different characteristics of chemically and structurally different spin labels have often been observed in the authors' lab. They make the application of ESR spectroscopy more versatile but need to always be taken into account for proper interpretation of results. The spectra for MTS-labeled residue 62 in the present data indicate that binding of F_1 to b_2 exerted a strong effect on the environment of the spin label. Surprisingly, the line width of the ESR spectra of spin-labeled *b*-residue 62 in the presence of F_1 was significantly narrower than in its absence, a result that strongly indicates that binding of F_1 allowed the radical more motional freedom, potentially by changing the overall structure of the protein surrounding the label.

ESR-spectra acquired in frozen solution to obtain interspin distances Acquiring ESR spectra in frozen solutions allows the detection of inter-spin dipolar interactions of up to about 25Å when using continuous wave ESR spectroscopy. Dipolar interactions are observed by line broadening of the resulting spectra which can then be used to determine interspin distances, for example as described in (Hustedt and Beth 1999; Hustedt et al. 2006). Figure 2a and b show

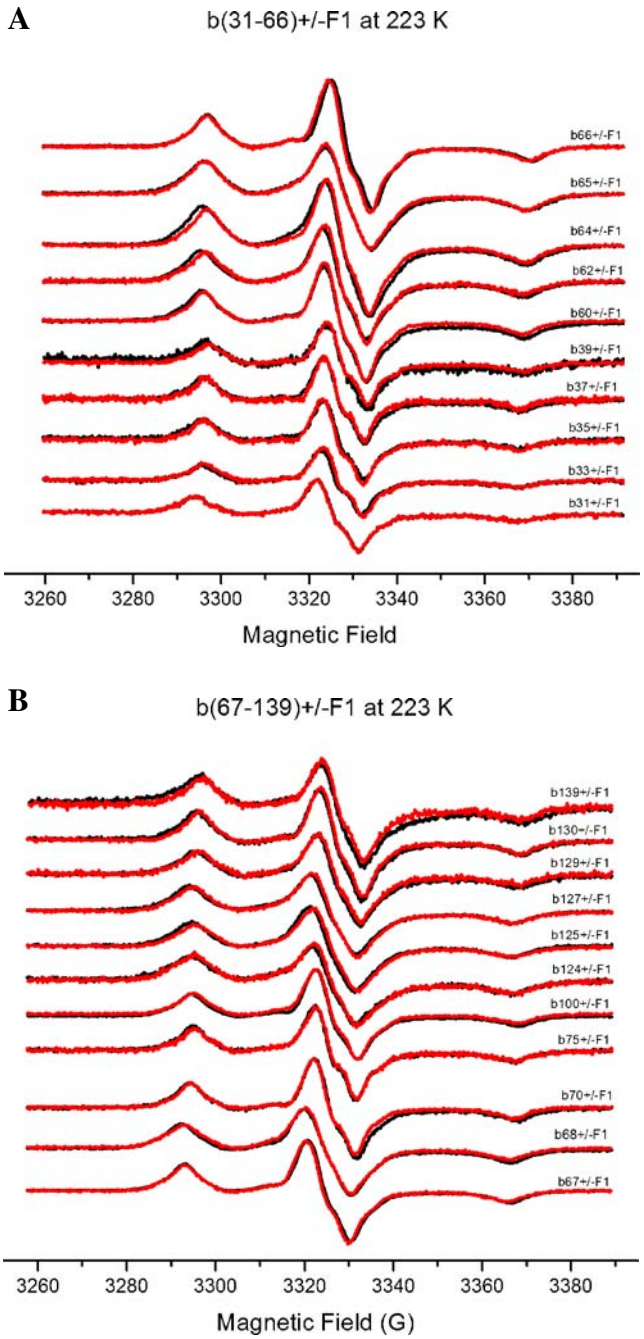

Fig. 2 ESR-spectra acquired in frozen solution of selected cysteine mutations in the E. coli F_oF_1-ATP synthase subunit b-dimer in the presence and absence of soluble F_1-ATPase. **a** ESR spectra of the same mutants shown in Fig. 1a within the tether domain of the subunit b-dimer were acquired at 223 K in frozen solution. **b** ESR spectra of spin-labeled b-mutants within the dimerization domain and towards the C-terminus acquired at 223 K. Again, the black lines represent the ESR spectra of the b-dimer alone; the overlaid red spectra were obtained after addition of a 1.2 fold excess of F_1-ATPase over b-dimer. The concentration of soluble subunit b-dimer was between 10 and 100 μM. Again, the corresponding spectra (+/− F_1) were normalized for their b-protein concentration to cancel out effects of dilution upon F_1 addition. Conditions for acquiring the ESR spectra are given in Experimental procedures

the frozen ESR spectra of the same set of MTS spin-labeled, truncated *b*-mutants as shown in Fig. 1, acquired at 223K, in the absence (black line) and presence (red line) of F_1-ATPase. Again, as above, no major changes were visible for the spectra of spin-labeled b_2 and in the determined interspin distances (see below) with or without F_1-ATPase, except in the range of residues 60 to about 64, where the spectra acquired in the presence of F_1 indicate a narrower line width than in the absence of F_1, indicative of less dipolar coupling of the adjacent spins and therefore of larger interspin distances.

Comparison of inter b-dimer interspin distances in the presence and absence of F_1-ATPase Similar to experiments reported in (Hornung et al. 2008) we compared the interspin distances derived form ESR analysis of the *E. coli b*-dimer to distances that were obtained by modeling the *b*-dimer as a left-handed coiled coil (Wise and Vogel 2008). Interspin distances from ESR experiments were determined using the program PAKERICH that was developed by Hustedt (Hustedt et al. 2006) in analogy to works by Steinhoff (Steinhoff et al. 1997) and Shin (Rabenstein and Shin 1995). The Chi-squared values of the fits were between 8.4 x 10^2 and 2.8 x 10^4 for all fits and differed depending on the protein concentrations and the resulting variations in the signal to noise ratios of the spectra. In Figure 3a we compare the interspin data in the absence of F_1 (Fig. 3a, red down arrows) to interspin distances derived from molecular modeling (black diamonds) as also described in (Hornung et al. 2008). Distances that were determined by ESR to be more than 25Å were set to 30Å and are shown as red stars unless they repeatedly gave values between 25 and 30Å or correlated well with the modeled distances (Hornung et al. 2008). Figure 3b shows the corresponding inter-*b*-distances when the truncated b-dimer was incubated in the presence of soluble F_1. Again the distances of the modeled *b*-dimer are shown as black diamonds and the ESR-determined distances are shown as red downward arrows or red stars. The interspin distances in the dimerization domain and closer to the C-terminal end of the *b*-dimer through to residue 139 are very similar in the presence and absence of the soluble ATPase (compare 3A to 3B). Large differences in the *b* to *b* interspin distances in the presence of F_1 are observed, however, in the tether domain from about residue 33 to residue 64. In this region the interspin distances observed in the presence of F_1 were larger than 25Å and could therefore not be measured accurately using continuous wave ESR spectroscopy (see red stars in Fig. 3b). These large interspin inter-b-distances are consistent with interspin distances from (Steigmiller et al. 2005) who determined the distances at amino acid positions 40, 51, 53, 62 and 64 to all be 29Å. These data

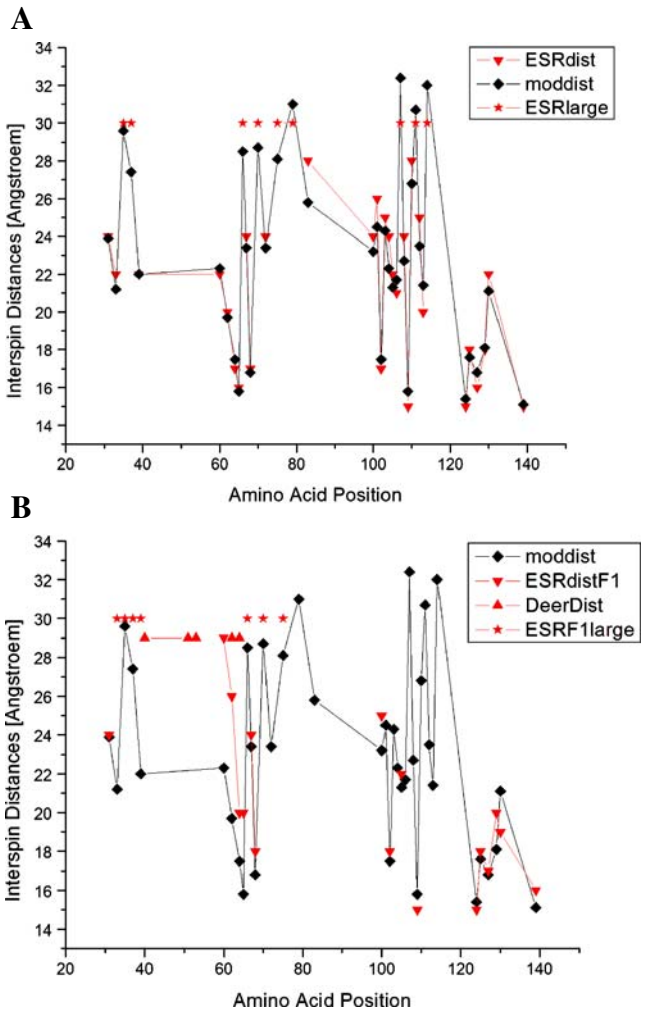

Fig. 3 *Interspin-distances of the b-dimer alone and in complex with soluble F_1-ATPase*. **a** Inter-spin distances of MTS-SL-labeled truncated *b*-dimers are compared that were derived from ESR experiments in frozen solution (red down arrows) or from molecular modeling the soluble *E. coli* subunit *b*-dimer as a left-handed non-staggered coiled coil (black diamonds) (Hornung et al. 2008). Such distances that were too large to be accurately determined by continuous wave ESR spectroscopy were set arbitrarily to 30 Å and are depicted as red stars. **b** The distances from ESR experiments in the presence of F_1 (red down arrows and red stars are compared to the distances of the modeled left-handed coiled coil (black diamonds). Similar distances within the tether domain of assembled F_oF_1-ATPase were observed using DEER ESR measurements as described in (Steigmiller et al. 2005). The data from (Steigmiller et al. 2005) are included in this Figure as red upward triangles

were included in Fig. 3b as red upward triangles for better comparison. The data suggest that in the presence of F_1 or in the complete F_oF_1-ATP synthase, the coiled coil that was predicted for the tether and dimerization domain of b_2 ((Hornung et al. 2008; Wise and Vogel 2008) opens and disengages in the lower tether region, while remaining intact in those regions that have been suggested for b_2 to interact with F_1 (Motz et al. 2004)

Discussion

The structure of the dimeric *b* external stalk of the bacterial F_oF_1-ATP synthase has been an enigma and grounds for controversy over the last couple of years. Reports were published that presented this seemingly simple protein dimer either as right-handed (Bi et al. 2008; Del Rizzo et al. 2002; Del Rizzo et al. 2006; Wood and Dunn 2007) or left-handed coiled coils (Hornung et al. 2008; Wise and Vogel 2008) (Volkov, O. A. , Zaida, T. M. , Voeller, P., Lill, H.,. Wise, J. G and Vogel, P. D., "*De-novo Modeling and ESR Validation of a Cyanobacterial F_{o1}-ATP Synthase Subunit bb' Left-handed Coiled Coil*", *submitted*; Wise, J. G. and Vogel P.D., "*Accommodating Discontinuities in Dimeric Left-handed Coiled Coils in ATP Synthase External Stalks*", *submitted*) or presented evidence that coiled coil formation at least in the tether domain seemed impossible due to relatively large inter-chain distances between the individual spin-labeled amino acids in the dimer (Steigmiller et al. 2005). Although the verdict on whether the protein adopts right-handed vs. left-handed coiled coils may still be out, this paper presents new evidence that shows that upon interaction of b_2 with the soluble F_1-ATPase, the tight coiled coil interaction of the dimer opens within the tether domain of subunit *b*, while the intact coiled coil packing remains in the subunit *b* dimerization domain. These new results explain and support many earlier findings as discussed here.

The tether domain between about residues 30 and 65 was thought not to interact directly with the $\alpha_3\beta_3$-ring (Motz et al. 2004). Insertions and deletions of several amino acids allowed formation of catalytically competent enzymes (Sorgen et al. 1998; Sorgen et al. 1999). Uneven length *b*-dimers (Bhatt et al. 2005; Grabar and Cain 2003; Grabar and Cain 2004) and even incorporation of non-*E. coli*-*b*-sequences (Claggett et al. 2007) also led to functional enzymes. These alterations to the proteins were usually made within this tether domain, and suggested great flexibility of the dimer in said domain. Also, early studies showed that the tether domain did not seem to contribute significantly to the dimerization interactions of the dimer (Dunn et al. 2000a; Dunn et al. 2000b).

We have employed in our studies site-specifically incorporated ESR active reporter groups, spin labels, into a soluble subunit *b*-dimer of *E. coli* ATP synthase where the membrane anchor had been removed and studied the respective ESR spectra in the absence and presence of soluble F_1. Room temperature ESR experiments showed that at residue 62 of subunit *b* a conformational transition took place upon binding of F_1. The resulting spectrum indicated greater mobility of the spin label in the presence of F_1 than in its absence (Fig. 1a). This result was surprising since typically the binding of a macromolecule

like the ATPase to a spin-labeled smaller molecule would be expected to result in loss of mobility of the radical due to increased rotational correlation times of the formed protein complex. The use of the relatively rigid and motionally restricted MTS spin label may, however, have lessened this overall effect on the spin-label mobility as compared to the previously employed, highly mobile IAAT spin label (Motz et al. 2004). The smaller line-width of MTS-labeled residue 62 in the presence of F_1 as compared to its absence strongly indicates a large conformational change within the protein has taken place that is consistent with disengagement and splitting up of a tight coiled coil packing in this region of b_2. ESR experiments in frozen solution (Fig. 2a and b) and subsequent extraction of interspin distances using dipolar broadening effects indeed showed that the inter-subunit inter-spin distances remained relatively constant in the dimerization domain (amino acids 65 to 139) when b_2 bound to F_1. In the region below amino acid 64, however, the dimer opened up to distances beyond the capability of continuous wave ESR. These distances were set by us to 30Å (Fig. 3b, red down arrows and red stars). The values that were obtained here are consistent with DEER measurements that indicated 29Å separation of spin-labeled residues in that same protein area and in the complete enzyme (Steigmiller et al. 2005) (added to Fig. 3b as red upward triangles). The findings are consistent with a dissociation and disengagement of the tether domain tight coiled coil packing (see Fig. 3a, red down arrows compared to black diamonds and (Hornung et al. 2008)) upon binding of F_1 (compare to red down arrows, red stars in Fig. 3b and compared to the black diamonds indicating the distances obtained through molecular modeling). This indicates that F_1-binding to the soluble *b*-dimer induces a similar conformational state as has been shown in the complete F_1F_o-ATP synthase. A cartoon depicting such a *b*-dimer interaction is shown in Fig. 4. With regard to earlier cross-link studies (Dmitriev et al. 1999) and (R. Priya, V. S. Tadwal, M. W. Roessle, S. Gayen, C. Hunke, W. C. Peng, J. Torres and G. Grüber, "Low resolution structure of subunit *b* (*b22–156*) of *Escherichia coli* F_1F_O-ATP synthase in solution and the *b*-δ assembly" (2008), *J. Bioenerg. Biomembr.,* Jul 31. [Epub ahead of print]), the transmembrane domain was arranged as closely packed parallel α-helices. The opening of the *b*-dimer is envisioned to be between the proline outside the membrane surface and about residue 64.

The presented studies suggest that even though the *E. coli* b_2 in solution is able to stably form a left-handed coiled coil, its structure changes significantly in the tether region when it binds to F_1. It seems reasonable that this region of b_2 may have evolved to open and disengage upon interaction with the rest of the enzyme. Further evidence for this requirement of the *b*-dimer to loosen its structure in the tether domain was found in our lab in recent studies of the heterodimeric *bb*' external stalk from a *Synechocystis* ATP synthase. At the same position within the stalk, about 30 amino acids from where the proteins are thought to leave the membrane, discontinuities in the heptad-repeat sequence were observed that lead to a looping out of four amino acid residues in the *b*' chain to then resume proper heptad packing with *b* and left-handed coiled coil formation C-terminal of this discontinuity. A model of the" looped-out" *bb*' was built as described in (Volkov, O. A., Zaida, T. M., Voeller, P., Lill, H., Wise, J. G and Vogel, P. D., "*De-novo Modeling and ESR Validation of a Cyanobacterial F_{o1}-ATP Synthase Subunit bb' Left-handed Coiled Coil*", *submitted*) and validated by ESR measurements using site specific spin labeling. Such a capability for loop formation in the tether domain may help explain the observation of unequal length *b*-subunits forming functional and active ATP synthases (Grabar and Cain 2003). It is intriguing to also note that this region of the external stalk likely exists as a single α-helical *b*-subunit tether in the divergent mitochondrial ATP synthase stalk, supported only by the C-terminal helix of f_6 (Dickson et al. 2006; Walker and Dickson 2006) that does not contain an membrane anchor, and may therefore allow for some flexibility.

Also suggestive for the requirement of a loosened coiled coil structure for functionality of the F_oF_1-ATP synthase are the recent results presented by the Dunn lab, where they showed that very tightly packing and perfectly canonical left-handed coiled coil sequences from leucine zipper

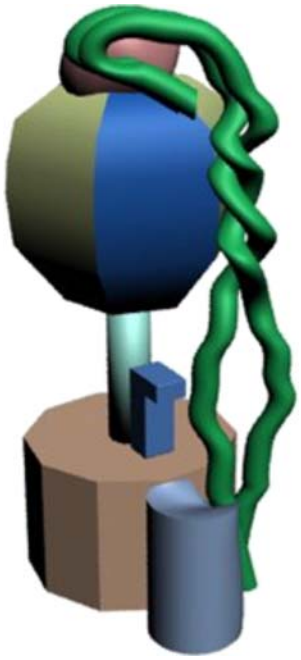

Fig. 4 *Cartoon of a potential arrangement of subunits b in the complete E. coli F_{o1}ATP synthase complex.* Taking into account previous data from (Dmitriev et al. 1999), (R. Priya, V. S. Tadwal, M. W. Roessle, S. Gayen, C. Hunke, W. C. Peng, J. Torres and G. Grüber, "Low resolution structure of subunit *b* (*b22–156*) of *Escherichia coli* F_1F_O-ATP synthase in solution and the *b*-δ assembly" (2008), *J. Bioenerg. Biomembr.*, Jul 31. [Epub ahead of print]), and data from this work, we have depicted the *b*-dimer as closely packed parallel α-helices that open and disengage presumably at the proline outside of the membrane. Close left-handed coiled coil packing then resumes C-terminal of amino acid 64

proteins, when substituted for normal *E. coli* sequences into the external stalk b_2 of *E. coli* ATP synthase at residues 55 through 110 resulted in several cases in an inactive chimeric enzyme (Bi et al. 2008). These mutations all included the region between residues 60 through 64 that we showed in this present report to undergo large conformational changes and opening of the dimer packing when interacting with the ATPase.

Our data suggest that the tight packing of the protein dimer resumes at amino acid 33, shortly before it enters the membrane. It was shown earlier that tight parallel packing interactions of b_2 exist in the membrane, see (Dmitriev et al. 1999) who showed disulfide cross-links with a periodicity of about 4 indicative of being on the same face of an α-helix over the span of residues 2–18 in the *b*-dimer in the absence of other subunits of the ATP synthase.

Dunn has suggested that a right-handed coiled coil packing might accommodate an elastic coupling mechanism of the *c*-ring rotation to the rotation of the γ-subunit since a potential unwinding of the left-handed coiled coil structure of γ could be counterbalanced with the winding or overwinding of a potential right-handed coiled coil in the *b*-dimer. To be elastic, this winding—overwinding of the right handed coiled coil has to raise its energy in a way that the gain in potential energy can be recovered when the system relaxes. One may argue, however, that the unwinding or overwinding of a b_2 left-handed coiled coil (depending on the catalysis direction) would accomplish the same function, namely, the potential energy of the over-or under-twisted left handed coiled coil would most likely be higher than in its canonically wound coiled coil ground state. Again, the increase in potential energy of the left-handed coiled coil upon rotation would also be available for return to the system upon relaxation of the strained twist. Indeed, any reversible disorganization of the dimer interface including dissociation or partial dissociation of the dimer could be used to store an energy input into the protein which could then be regained upon relaxation to the fully folded, dimeric ground state.

In light of the results presented here it is interesting to speculate on the possible role of elastic transient energy storage within the external stalk of the enzyme during turnover. If the b_2 structure in the dimerization domain that has been shown to interact with F_1 (residues >80 in *b*) (Motz et al. 2004) remains as an unperturbed coiled coil and demonstrates the complementarity when bound to F_1 that the recent mitochondrial external stalk demonstrates (Dickson et al. 2006; Walker and Dickson 2006), then it might be assumed that this region of the stalk remains still and inflexible. If so, then only the transmembrane region and the regions of the tether (residues 31–64) and the remainder of the dimerization domain (residues 65–79) would be available for elastic storage and return of free energies of conformational change during catalysis. In this scenario, any twisting, winding, unwinding or stretching of the potential coiled coil regions of the bacterial b_2 would be functionally equivalent to similar high energy states imparted to the mitochondrial *b-f6-d* complex. If these are specific conformational changes dependent on coiled coil structures in the bacterial enzyme, then evolutionary divergence in the mitochondrial enzyme would have had to replicate the subtle effects of coil over-or underwinding with the very different *b-f6-d* structures. A simpler evolutionary divergence situation would exist if the requirement for elastic energy return was not dependent on the coiled coil structure or if the external stalk did not function in elastic energy returns during turnover.

It will be of great interest to further investigate the structural and mechanistic implications of the unusual "bubble"-structure in the *b*-dimer within the tether domain in the F_1 and F_1F_o complexes.

Acknowledgments The authors wish to thank Stanley D. Dunn, University of Western Ontario, Canada, for providing the plasmid pDM3 and plasmids for some of the mutant *b*-proteins used in this work, and Alan E. Senior, University of Rochester School of Medicine, for strain SWM1. We also wish to thank Eric J. Hustedt for providing us with the program PAKERICH to extract interspin distances from dipolar broadening of ESR spectra.

References

Bhatt D, Cole SP, Grabar TB, Claggett SB, Cain BD (2005) Manipulating the length of the b ubunit F1 binding domain in F1F0 ATP synthase from Escherichia coli. J Bioenerg Biomembr 37:67–74

Bi Y, Watts JC, Bamford PK, Briere LK, Dunn SD (2008) Probing the functional tolerance of the b subunit of Escherichia coli ATP synthase for sequence manipulation through a chimera approach. Biochim Biophys Acta

Claggett SB, Grabar TB, Dunn SD, Cain BD (2007) Functional incorporation of chimeric b subunits into F1Fo ATP synthase. J Bacteriol 189:5463–5471

Del Rizzo PA, Bi Y, Dunn SD (2006) ATP synthase b subunit dimerization domain: a right-handed coiled coil with offset helices. J Mol Biol 364:735–746

Del Rizzo PA, Bi Y, Dunn SD, Shilton BH (2002) The "second stalk" of Escherichia coli ATP synthase: structure of the isolated dimerization domain. Biochemistry 41:6875–6884

Dickson VK, Silvester JA, Fearnley IM, Leslie AGW, Walker JE (2006) On the structure of the stator of the mitochondrial ATP synthase. EMBO J 25:2911–2918

Dmitriev O, Jones PC, Jiang W, Fillingame RH (1999) Structure of the membrane domain of subunit b of the Escherichia coli FoF1 ATP synthase. J Biol Chem 274:15598–15604

Dunn SD, McLachlin DT, Revington M (2000a) The second stalk of Escherichia coli ATP synthase. Biochim Biophys Acta 1458:356–363

Dunn SD, Revington M, Cipriano DJ, Shilton BH (2000b) The b subunit of Escherichia coli ATP synthase. J Bioenerg Biomembr 32:347–355

Grabar TB, Cain BD (2003) Integration of b subunits of unequal lengths into F1F0-ATP synthase. J Biol Chem 278:34751–34756

Grabar TB, Cain BD (2004) Genetic complementation between mutant b subunits in F1F0 ATP synthase. J Biol Chem 279:31205–31211

Hornung T, Volkov OA, Zaida TMA, Delannoy S, Wise JG, Vogel PD (2008) Structure of the Cytosolic Part of the Subunit b-Dimer of Escherichia coli FoF1-ATP Synthase. Biophys J 94:5053–5064

Humphrey W, Dalke A, Schulten K (1996) VMD: visual molecular dynamics. J Mol Graph 14:33–8, 27–8

Hustedt EJ, Beth AH (1999) Nitroxide spin-spin interactions: applications to protein structure and dynamics. Annu Rev Biophys Biomol Struct 28:129–153

Hustedt EJ, Stein RA, Sethaphong L, Brandon S, Zhou Z, Desensi SC (2006) Dipolar coupling between nitroxide spin labels: the development and application of a tether-in-a-cone model. Biophys J 90:340–356

Junge W, Pänke O, Cherepanov DA, Gumbiowski K, Müller M, Engelbrecht S (2001) Inter-subunit rotation and elastic power transmission in F0F1-ATPase. FEBS Lett 504:152–160

Laemmli UK (1970) Cleavage of structural proteins during the assembly of the head of bacteriophage T4. Nature 227:680–685

McDonnell AV, Jiang T, Keating AE, Berger B (2006) Paircoil2: improved prediction of coiled coils from sequence. Bioinformatics 22:356–358

McLachlin DT, Dunn SD (1997) Dimerization interactions of the b subunit of the Escherichia coli F1F0-ATPase. J Biol Chem 272:21233–21239

Motz C, Hornung T, Kersten M, McLachlin DT, Dunn SD, Wise JG, Vogel PD (2004) The subunit b dimer of the FoF1-ATP synthase: interaction with F1-ATPase as deduced by site-specific spin-labeling. J Biol Chem 279:49074–49081

Ousterhout J (1994) Tcl and the Tk Toolkit. Addison-Wesley Professional, Upper Saddle River, NJ

Rabenstein MD, Shin YK (1995) Determination of the distance between two spin labels attached to a macromolecule. Proc Natl Acad Sci U S A 92:8239–8243

Sanner MF (1999) Python: a programming language for software integration and development. J Mol Graph Model 17:57–61

Schaftenaar G, Noordik JH (2000) The effect of isodensity surface sampling on ESP derived charges and the effect of adding bondcenters on DMA derived charges. J Comput Aided Mol Des 14:233–242

Schmidt MW, Baldridge KK, Boatz JA, Elbert ST, Gordon MS, Jensen JH, Koseki S, Matsunaga N, Nguyen KA, Su S, Windus TL, Dupuis M, Montgomery JA (1993) General Atomic and Molecular Electronic Structure System. J. Comput. Chem 14:1347–1363

Schwieters CD, Kuszewski JJ, Tjandra N, Clore GM (2003) The Xplor-NIH NMR molecular structure determination package. J Magn Reson 160:65–73

Sorgen PL, Bubb MR, Cain BD (1999) Lengthening the second stalk of F(1)F(0) ATP synthase in Escherichia coli. J Biol Chem 274:36261–36266

Sorgen PL, Caviston TL, Perry RC, Cain BD (1998) Deletions in the second stalk of F1F0-ATP synthase in Escherichia coli. J Biol Chem 273:27873–27878

Steigmiller S, Börsch M, Gräber P, Huber M (2005) Distances between the b-subunits in the tether domain of FoF1-ATP synthase from E. coli. Biochim Biophys Acta 1708:143–153

Steinhoff HJ, Radzwill N, Thevis W, Lenz V, Brandenburg D, Antson A, Dodson G, Wollmer A (1997) Determination of interspin distances between spin labels attached to insulin: comparison of electron paramagnetic resonance data with the X-ray structure. Biophys J 73:3287–3298

Taussky HH, Shorr E (1953) A microcolorimetric method for the determination of inorganic phosphorus. J Biol Chem 202:675–685

Vik SB (2007) ATP Synthesis by Oxidative Phosphorylation

Walker JE, Dickson VK (2006) The peripheral stalk of the mitochondrial ATP synthase. Biochim Biophys Acta 1757:286–296

Wise JG (1990) Site-directed mutagenesis of the conserved beta subunit tyrosine 331 of Escherichia coli ATP synthase yields catalytically active enzymes. J Biol Chem 265:10403–10409

Wise JG, Vogel PD (2008) Subunit b-dimer of the Escherichia coli ATP synthase can form left-handed coiled-coils. Biophys J 94:5040–5052

Wood KS, Dunn SD (2007) Role of the asymmetry of the homodimeric b2 stator stalk in the interaction with the F1 sector of Escherichia coli ATP synthase. J Biol Chem 282:31920–31927